Atomic Force Microscope-Related Study Membrane-Associated Cytotoxicity in Human Pterygium Fibroblasts Induced by Mitomycin C

Xiaofang Cai,[†] Xiaoxi Yang,[‡] Jiye Cai,*[,†] Shixian Wu, and Qian Chen[†]

Department of Chemistry, The First Affiliated Hospital, Jinan University, Guangzhou, Guangdong 510632, People's Republic of China,

Received: November 10, 2009; Revised Manuscript Received: January 9, 2010

Mitomycin C (MMC) has been shown to have a therapeutic effect against human pterygium fibroblasts (HPFs) by inducing apoptosis. However, there is little data about the effect of it on plasma membrane. In the present study, the cytotoxicity of MMC to HPFs including inhibiting cell growth, inducing apoptosis and bringing about membrane toxicity was investigated. It was found that MMC could significantly suppress the proliferation of HPFs in a dose-dependent manner by CCK-8 assay. Flow cytometric analysis also revealed that treatment with MMC resulted in increased percentages of apoptotic cells in a dose-dependent manner. Membrane lipid peroxidation level, lactate dehydrogenase (LDH) leakage, membrane surface topography, and membrane rigidity alterations were investigated to assess the membrane toxicity induced by MMC. Treatment with MMC at different concentrations accelerated membrane lipid peroxidation and potentiated LDH leakage, which was consistent with disturbance of membrane surface and decrease of membrane elasticity detected by atomic force microscopy. All the above changes led to the disturbed intracellular Ca^{2+} homeostasis, which was an important signal triggering apoptosis. Hence, the membrane toxicity induced by MMC might play an important role in the process of apoptotic induction and the calcium channel may be one of the apoptosis mechanisms.

Introduction

Mitomycin C (MMC) is an antimitotic agent. It prevents cell replication by forming irreversible bonds between the two strands of the DNA helix and induces apoptosis.[1] Its use is based on its ability to suppress ocular fibroblastic activity, which is responsible for the subconjunctival proliferation and fibrosis that characterize pterygium.[2] Pterygium, a common pathologic alteration of the ocular surface, is a progressive fibrovascular overgrowth from the conjunctiva onto the cornea.[2]

In a previous study, MMC was demonstrated to induce apoptosis of HPFs in vivo.[3] However, little is known about AFM detection of the image and mechanics of HPFs. There is no available information concerning the influence of MMC on plasma membrane concomitant with its apoptotic induction.

In recent years, a number of studies have employed AFM to study the image[4−7] and mechanical properties of the living cell.[8−13] Mechanical properties of cells are becoming recognized as indicators and regulators of physiological processes such as differentiation, malignant phenotypes, and mitosis.[14−16] Research into biomechanics at the cellular and molecular levels of some human diseases has not only led to a better elucidation of the mechanisms behind disease progression but has also provided important knowledge for fighting against these diseases.

Membrane is thought to be involved in diverse cellular functions, particularly signal transduction. Previous research showed that extracellular membrane polysaccharides play a crucial role in determining the surface elasticity.[14] The cytoskeleton was also involved with the mechanical properties of cells,[16−18] as well as membrane rafts this kind of nanoclusters that make the mechanical properties of cells different.[19−21] Previous data also showed that the mechanics were also related to cell surface brush.[22]

Plasma membrane constitutes the boundary between a living cell and its environment and plays an important function in controlling the transport of ions. Disturbance of the membrane structure as well as changes of membrane characteristics will lead to functional alteration of the membrane, particularly the transport and flux of Ca^{2+} through membrane channels, which may trigger the apoptotic signal pathway.[23] We speculate that during the entrance process into pterygium cells, MMC can interact with the membrane phospholipids or proteins, rendering the alteration of biological and physical characteristics of the plasma membrane and subsequently leading to the disturbance of cellular homeostasis and even apoptosis.

In the present study, the growth inhibition and apoptosis of HPFs were assessed. In addition, membrane toxicity was investigated, including membrane image conformation and mechanics, membrane integrity alteration, membrane oxidative injury. Furthermore, intracellular free Ca^{2+} alteration in HPFs following MMC exposure was also examined.

Materials and Methods

Reagents. Mitomycin-C for injection (MMC) was purchased from Zhejiang Hisun Pharmaceutical Co. Ltd. It was dissolved in ultrapure water and diluted with DMEM. RPMI 1640 medium and newcalf serum were purchased from Hangzhou Sijiqing Biological Engineering materials Co., Ltd. Cell Counting Kit (CCK-8) was purchased from Dojin Laboratory (Kumamoto, Japan). Lactate dehydrogenase (LDH) and a Malondialdehyde (MDA) detection kit were purchased from Nanjing Jiang Cheng Bioengineering Institute, China. Fluo-3 AM was purchased from Beyotime institute of biotechnology, China. A Annexin V-FITC/PI apoptosis detection kit was purchased from Keygen biotechnology, China.

* To whom correspondence should be addressed. E-mail: tjycai@jnu.edu.cn. Tel./Fax: +86 20 8522 3569.
[†] Department of Chemistry.
[‡] The First Affiliated Hospital.

10.1021/jp910682q © 2010 American Chemical Society
Published on Web 03/02/2010

Cell Culture. Pterygium was obtained from department of Ophthalmology, The First Affiliated Hospital of Jinan University. Pterygium specimens were obtained after the surgical removal of primary pterygium. The central portion of the pterygium body was used for culture. The specimen was cut into explants of approximately 1 × 1 mm and placed onto 100 mm tissue culture dishes. Ten minutes later, each explant was covered with a drop of FBS and placed in an incubator at 37 °C under 95% humidity with 5% CO_2 for 4 to 6 h. Ten milliliters of DMEM medium enriched with 10% FBS, 100 U/ml penicillin, and 0.1 mg/mL streptomycin was added afterward, and the medium was changed every 2 days thereafter. Fibroblasts were subcultured with 0.25% trypsin and 0.02% EDTA in a calcium-free MEM medium at 80 to 90% confluence with a 1:2 to 1:3 split for three passages. Exponentially growing cells were used throughout the study. Two × 10^5 HPFs were cultured in various concentrations of MMC (50, 100, 200, 300, and 400 μg/mL) for 12 h.

Cell Proliferation Assay. Cell viability was assessed by a Cell Counting Kit (CCK-8). One × 10^4 HPFs were plated on a 96-well microplate (200 ul/well). MMC at various concentrations were added, and the final concentrations are 0, 50, 100, 200, 300, and 400 μg/mL, respectively. The plate was incubated in humidified air at 37 °C with 5% CO_2 for 12 h. Twenty microliter solutions containing WST-8 were added to each well and were incubated for an additional 2 h. The absorbance was measured at 450 nm on an automated microplate reader (TECAN Model Safire2). Inhibition rate = $[1 - OD_{control}/OD_{treatment}] \times 100\%$

Determination of Apoptosis Rate. An Annexin V-FITC/PI apoptosis detection kit was used to detect early apoptotic activity according to the manufacturer's instructions, with slight modifications. The cells were seeded at 2 × 10^5 cells per well in 6-well plates. After treatment with 0, 50, 100, 200, and 300 μg/mL of MMC for 12 h, the cells were harvested and washed twice with ice-cold phosphate-buffered saline (PBS) and resuspended in 500 μL of binding buffer. A total of 5 μL of Annexin V-FITC and 5 μL of propidium iodide (PI) were added and the mixture was incubated for 30 min in the dark. Finally, 400 μL of binding buffer was added to the cells, the mixtures were analyzed with a Flow cytometer (FACSCalibur, Becton Dickinson), using an FITC signal detector (FL1), and PI signal detector (FL2). The apoptotic percentage of 5000 cells was determined, after which all the experiments reported in this study were performed 3 times. The data were analyzed using Cell Quest software (Win MDI) for calculation of percentage cells with apoptosis per group.

Determination of Lipid Peroxides. Total lipid peroxidation in HPFs was determined by the amount of malondialdehyde (MDA), the final product of lipid peroxidation. Briefly, after treatment with various concentrations of MMC (0, 50, 100, 200, and 300 μg/mL) for 12 h, cells were collected and washed twice with PBS. The MDA concentration was measured using MDA detection kit according to the manufacturer's instructions. At last, the cells were seeded in 96-well plates for automated microplate reader (TECAN Model Safire2). The absorbance was measured at 532 nm.

Lactate Dehydrogenase (LDH) Leakage Assay. Extracellular LDH levels were used as an indicator of membrane permeability. Briefly, after treatment with various concentrations of MMC (0, 50, 100, 200, and 300 μg/mL) for 12 h, cells were collected and washed twice with PBS. The percentage of LDH release into the medium was measured using LDH detection kit according to the manufacturer's instructions. At last, the cells were seeded in 96-well plates for automated microplate reader (TECAN Model Safire2). The absorbance was measured at 440 nm.

Atomic Force Microscopy (AFM) Analysis. An Autoprobe Cp AFM (thermomicroscope) was used in contact mode to perform the topographic images and AFM-based force spectroscopy was used to perform the force detection. Force−distance curves were obtained through standard retraction. All force−distance curve experiments were performed at the same loading rate. The curvature radius of the silicon tip is less than 10 nm, as for the tips used in the contact mode, the length, width, and thickness of cantilever are 115, 30, 3.5 mm, respectively, the oscillation frequency is 255 kHz, and the force constant is 0.01 N/m.

Young's Modulus Calculation from Hertz Models. Young's modulus calculations, based on the basic Hertz model,[24,25] were done on samples of control and apoptosis HPFs to compare the impact of these states on the calculated modulus. These models show the relationship between the applied force F and the indentation δ, as shown in the following equation

$$F = \frac{4}{3}\frac{E}{1-\nu^2}\sqrt{R\delta^3}$$

where ν is the Poisson ratio, F is the loading force, δ is the indentation, E is the Young's modulus, and R is the radius of the curvature of the AFM tip, respectively. A Poisson ratio of 0.5 is appropriate for lipid bilayers, cells, and vesicles. The sample indentation, δ, is defined as the difference between the piezo translation and the cantilever deflection since there is an indentation in the sample caused by its softness. An indentation of only 10% of the total sample thickness was considered for the calculation to limit the influence from the underlying substrate.[24]

Intracellular Free Ca^{2+} Detection. Intracellular Ca^{2+} detection of HPFs was performed after cells were exposed to MMC (0, 50, 100, 200, 300 μg/mL) for 12 h. In brief, cells planted into 6-well plates were loaded with 5 μmol/L Fluo-3 AM in hepes buffer (10 mmol/L, pH 7.4). The plate was incubated in humidified air at 37 °C with 5% CO_2 for 1 h. Cells were collected and washed twice with PBS. The resulting fluorescence as the indicator of Ca^{2+} concentration was observed under with the Flow cytometer (FACSCalibur, Becton Dickinson) at excitation wavelength 488 nm, emission wavelength 525 nm. The data were analyzed using Cell Quest software (Win MDI) for calculation of Ca^{2+} concentration per group.

Statistical Analysis. All the experiments were replicated at least three times. Data were presented as mean ± standard deviation and analyzed using Student's t test. A p-value of <0.05 was considered statistically significant.

Results and Discussion

Effects of MMC on the Growth of HPFs. The effects of MMC on the growth of HPFs were examined by the CCK-8 assay. As shown in Figure 1, exposure to MMC (0, 50, 100, 200, 300, and 400 μg/mL) for 12 h resulted in a significantly inhibitory effect on the growth of HPFs in a dose-dependent manner. As the concentration of MMC increased, the inhibition rate obviously increased. The data confirmed that MMC ($\geq$100 μg/mL) can inhibit the growth of HPFs.

Effects of MMC on Apoptosis Induction in HPFs. To assess whether the growth inhibition by MMC was caused by induction of apoptosis, flow cytometry was used to quantify

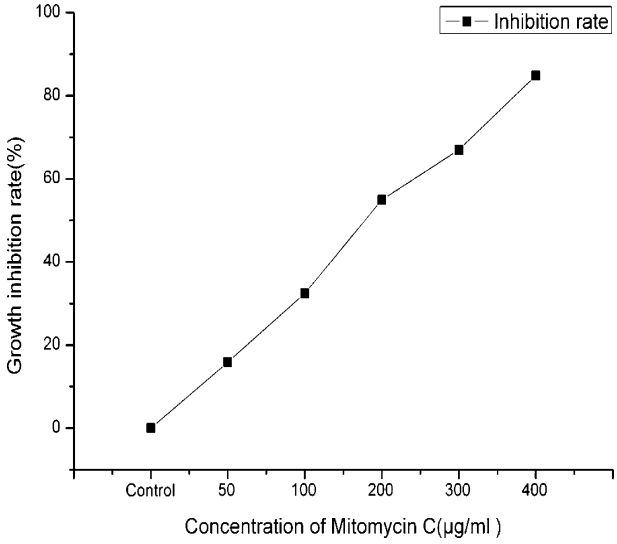

Figure 1. Inhibitory effects on the growth of HPFs exposed to MMC for 12 h. Comparing treated cell group with the control group, When the concentration of MMC was up to 200 μg/mL, the inhibition rate was >50%. As the concentration of MMC increased, the cell growth inhibition rate increased significantly. Control group meant the cells were not treated with MMC.

the percentage of apoptotic cells exposed to MMC for 12 h. As seen in Figure 2, Q4 represented the early apoptosis of cells. The percentages of apoptotic cells were 4.2, 4.2, 5.4, 19.3, and 25.8%, corresponding to 0, 50, 100, 200, and 300 μg/mL, respectively. The apoptosis of 200 μg/mL group was obviously higher than control group. In accord with Figure 1, the data showed that MMC ($\geq$200 μg/mL) can inhibit the HPFs growth and induce apoptosis.

AFM Image Analysis. Each cell has its specific size and shape, which plays a specific function. Once the cells cannot maintain the inherent shape, its function would be jeopardized, which would bring a range of issues.[26] Knowing about HPFs surface images is the key to understand their functions. To gain a comprehensive structure of HPFs, they were analyzed using AFM topographic imaging.

With this in mind, we first investigated the surface structure of the two HPFs morphotypes using AFM. As shown in Figure 3[3], the AFM images of HPFs revealed a remarkable difference in cell surface architecture in the absence (Figure 3 a−h) and presence of MMC (Figure 3A−G). For the control group, AFM image revealed a typical long spindle-shaped fibrocyte (Figure 3a−d). The tail unrolled and presented threadiness (Figure 3f). There were some pores in the tail (Figure 3e). The cell surface was smooth (Figure 3g). For the 200 μg/mL group, the cell also presented long spindle-shaped fibrocyte (Figure 3A−B). The tail rolled and presented no threadiness (Figure 3C−E). The pores in the tail disappeared. Nanoparticles appeared a lot on the membrane (Figure 3F−G). It has been reported that the visible protruding particles are clusters of membrane proteins, indicating a disorganized topographic structure of the membrane. These AFM images provided an evidence for the toxic effects of MMC on HPFs membrane.

Nanomechanical Properties of the HPFs. Previous studies revealed that cell morphology will affect adhesion.[27,28] It suggests difference in morphology may also lead to difference in their mechanical properties. The interaction between medicament and the cell can induce changes in mechanical properties of the cell.[29,30]

Here we used AFM force spectroscopy to probe the nanomechanical properties to extract Young's modulus of control and apoptosis groups, respectively. Nucleoli were chosen as nucleus points because it was easy to align the cantilever sphere over it, allowing data collection on the very same spot over the experiment and avoiding drifting or changes due to cell

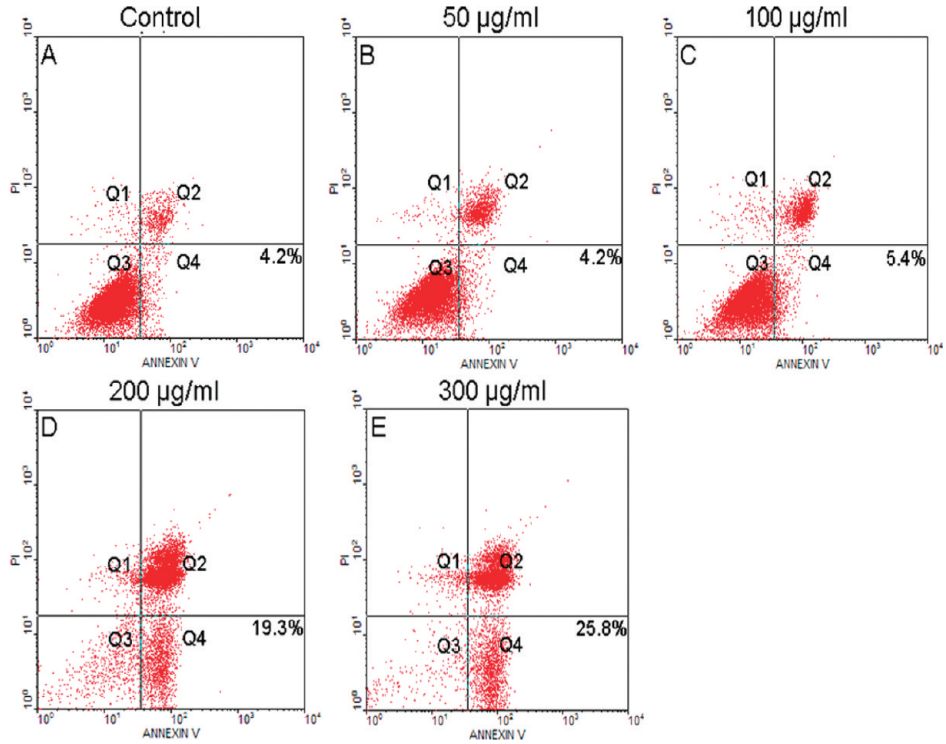

Figure 2. Flow cytometric analysis of apoptosis in HPFs exposed to MMC. The cells were treated with various concentrations of MMC (0, 50, 100, 200, and 300 μg/mL) for 12 h. (A) Control group, (B) 50 μg/mL, (C) 100 μg/mL, (D) 200 μg/mL, (E) 300 μg/mL. The percentage shown in Q4 was the percentages of early apoptosis cells. As the concentration of MMC increased, the cell apoptosis rate increased significantly. Control group meant the cells were not treated with MMC.

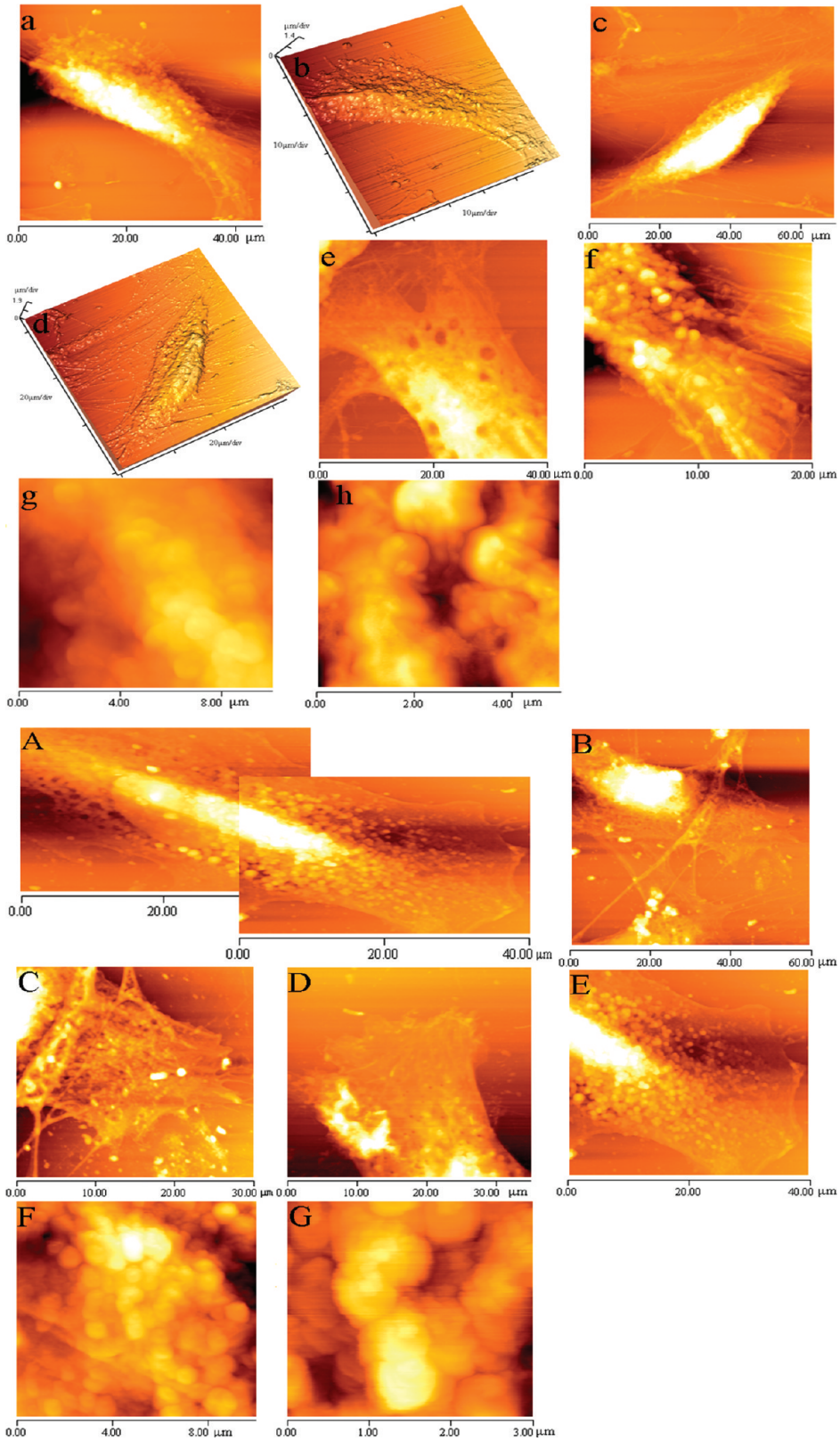

Figure 3. AFM images of HPFs, control and 200 μg/mL group, respectively. (a−h) Control group, (a−d) the whole cell image; size, 45 × 45 μm, 70 × 70 μm. (e−f) Tail image, size: 40 × 40 μm, 20 × 20 μm. (g−h) ultrastructure image, size: 10 × 10 μm, 5 × 5 μm. (A−G) 200 μg/mL group, (A−B) the whole cell image, size: 70 × 70 μm, 60 × 60 μm. (C−E) tail image, size: 30 × 30 μm, 35 × 35 μm, 40 × 40 μm. (F−G) ultrastructure image, size: 10 × 10 μm, 3 × 3 μm.

movements, such as contraction.[31] Force−distance mages consisting of arrays of 16 × 16 force curves were recorded in parallel with topographic images. Figure 4 shows elasticity maps of the two strains and elasticity histograms recorded on top of the cells membrane. Most curves were well-described by the Hertz model, allowing us to obtain Young's modulus values. Elasticity maps obtained at the control group showed the average Young's modulus being 4.7 ± 1.9 kPa (Figure 4B). Notably, elasticity maps recorded on the apoptosis group (200 μg/mL) clearly showed contrast, the average Young's modulus being

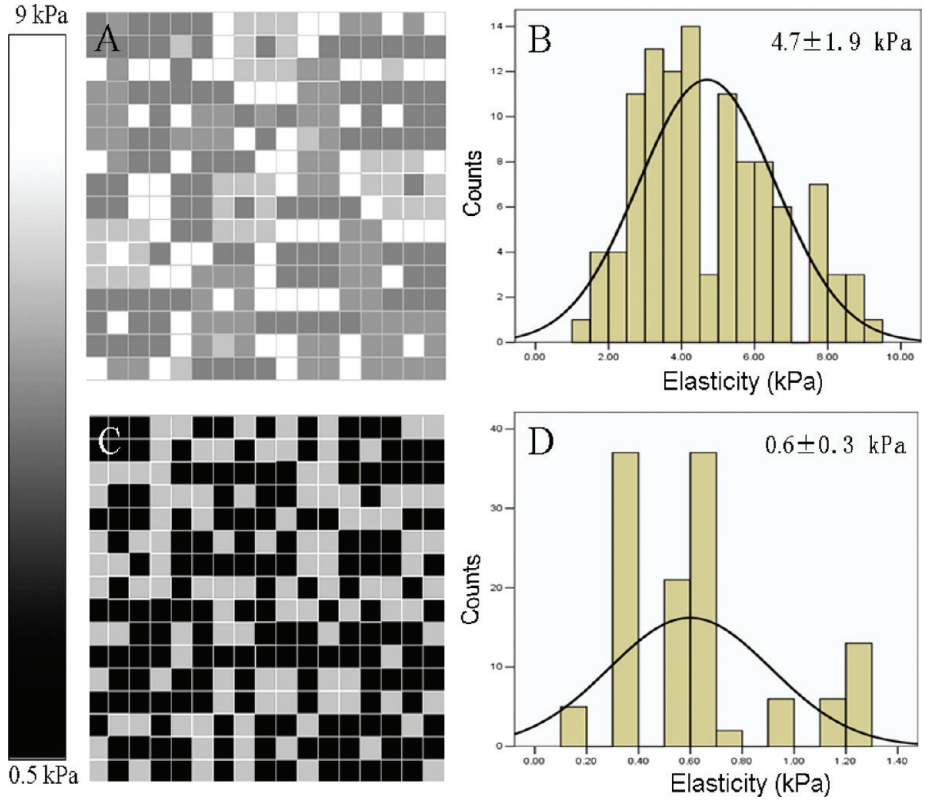

Figure 4. Elasticity maps (A and C) and elasticity histograms (B and D) resulted from force−distance curves on top of untreated HPFs and treated HPFs, respectively. In the elasticity map, white color corresponds to large Young's Modulus and black color corresponds to the low Young's modulus. The frequency was constructed from an ensemble of Young's modulus. The maximum of the frequency depicted the most probable elasticity. (A−B) The elasticity of untreated HPFs distributed in 4.7 ± 1.9 kPa. (C−D) The elasticity of treated HPFs distributed in 0.6 ± 0.3 kPa.

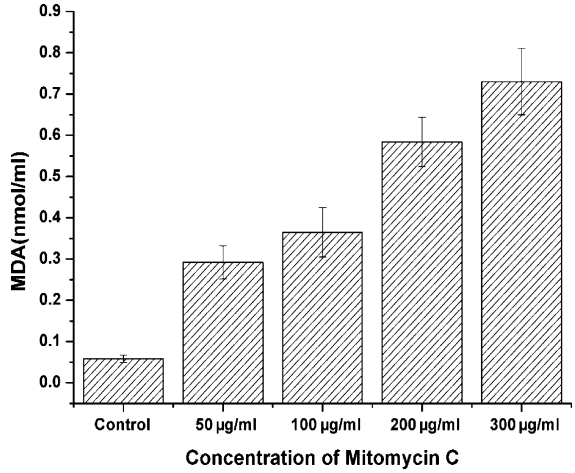

Figure 5. Effects on the level of membrane lipid peroxidation expressed with MDA in HPFs exposed to MMC for 12 h. After treatment with various concentrations of MMC (0, 50, 100, 200, and 300 μg/mL) for 12 h, the absorbance of samples was recorded at 532 nm, respectively.

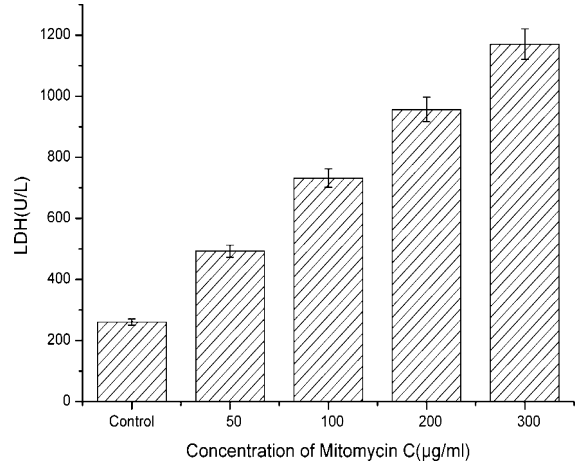

Figure 6. LDH assay for membrane permeability detection. After HPFs were treated with (0, 50, 100, 200, and 300 μg/mL) MMC for 12 h, LDH in the culture medium was detected. Data are presented as mean ± SD.

0.6 ± 0.3 kPa (Figure 4D). The apoptosis HPFs appears 70% softer compared to the control group, a finding that may identify with differences in cell membrane morphology.

In our study, after treatment with MMC, the membrane lipid component of the HPFs may be altered, or the membrane fluidity changed, or the cytoskeleton under the membrane altered. Any of these changes may be responsible for the different mechanics. Composition and structural changes in erythrocyte membranes and compositional changes in plasma lipids may contribute to the mechanics.

In order to further elucidate the cytotoxicity of MMC, changes in membrane oxidative damage, membrane permeability and intracellular free Ca^{2+} concentration assessed by assays of lipid peroxidation, LDH leakage and Fluo-3 AM were also investigated in the following study, respectively.

Effects of MMC on Membrane Lipid Peroxidation in HPFs. Data presented in Figure 5 showed the results of the membrane lipid peroxidation level (expressed as MDA) in HPFs treated with MMC for 12 h. Compared with the control group, exposure to MMC caused a significant increase in MDA concentration in a dose-dependent manner. Even under the

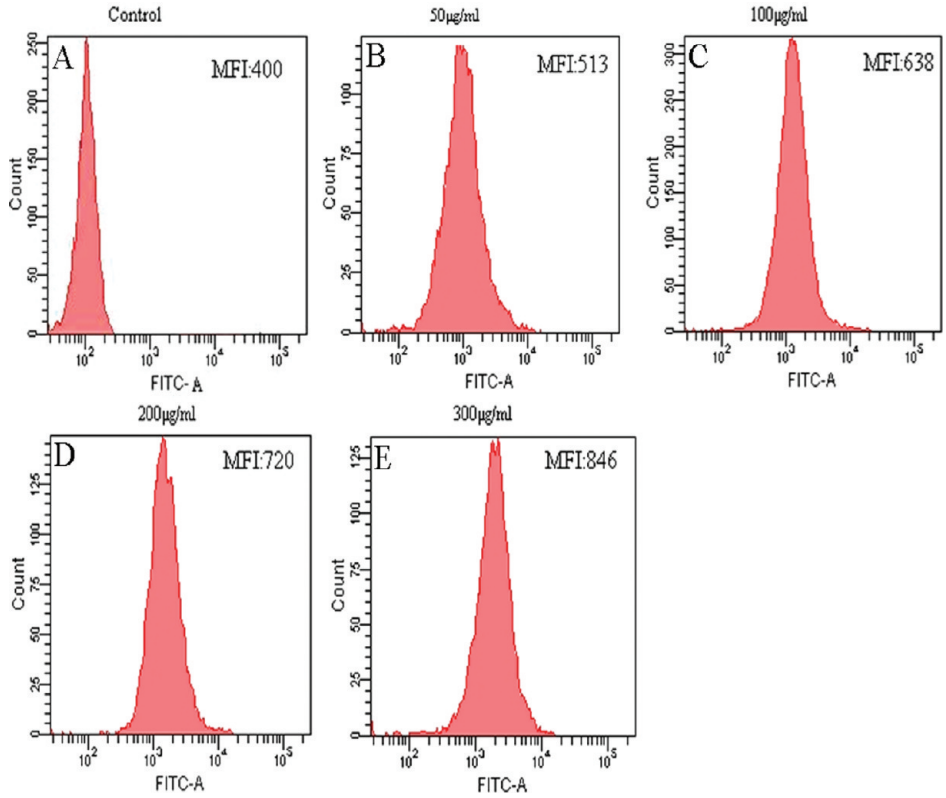

Figure 7. Changes of intracellular free Ca^{2+} measured in HPFs incubated with MMC (0, 50, 100, 200, and 300 μg/mL) for 12 h. The result showed that MMC induced a dose-dependent elevation of cytosolic free Ca^{2+}. Ca^{2+} concentrations in MMC-treated cells exhibited significantly different as compared with the control. MFI means the mean fluorescence intensity. Fluorescence intensity represents the Ca^{2+} concentration. The left axis is the cell number.

concentration of 100 μg/mL exposure, which was not enough to induce apoptosis, a significant enhancement in the level of lipid peroxidation, was observed in HPFs compared with the control group.

It is well-known that plasma membranes are made up of phospholipid molecules with various large globular protein molecules suspended in them, sometimes coated with carbohydrates (sugars). Because of the high polyunsaturated fatty acid content, plasma membranes are highly sensitive to reactive oxygen species $(ROS)^-$ induced damage. ROS, including superoxide (O^{2-}) and hydroxyl radicals ($\cdot OH$) and hydrogen peroxide (H_2O_2), have been demonstrated to be implicated with the induction of apoptosis.[32,33] Excessive ROS may attack biological macromolecules, including lipid, protein, and DNA strands, leading to oxidative damage of which membrane lipid peroxidation is one of the primary indicators.[34] Lipid peroxides are more hydrophilic than their undamaged, unsaturated lipid counterparts; these molecules can disrupt membrane structure and function, thereby increasing membrane permeability.[35]

On the basis of the results, it is also implied that the membrane lipid peroxidation level may be a sensitive responser to cytotoxicity. Because lipid peroxides are more hydrophilic than their undamaged, unsaturated lipid counterparts, these molecules can disrupt membrane structure and function, thereby increasing membrane permeability.

Effects of MMC on Membrane Permeability in HPFs. Release of LDH into the culture medium was measured to assess MMC effect on the membrane permeability of HPFs. Figure 6 showed that augmented membrane permeability induced by MMC in dose-dependent manners. Consistent with the promotion of lipid peroxidation, higher concentration MMC induced more significant effect. Results from the current study demonstrated that MMC may destabilize the membrane structure, resulting in the release of membrane components and a concomitant enhancement of permeability. The increase in the activity of MDA (Figure 5) and LDH (Figure 6) might be attributed to the disturbance of the membrane organization (Figures 3 and 4). Increased membrane permeability can produce a breakdown of transmembrane ion gradients and inhibition of integrated cellular metabolic processes.

Intracellular Free Ca^{2+} Studies. Intracellular calcium levels are normally maintained at micromolar levels in cells. It is due to a balance between calcium influx through voltage-dependent channels and calcium efflux by active transport systems or through sequestration of calcium in the endoplasmic reticulum (ER). In our present study, elevated intracellular Ca^{2+} concentration was also observed (Figure 7), which demonstrated that ion fluxes were altered. Disturbance of Ca^{2+} homeostasis may trigger diverse cellular processes, even apoptosis.

The rise in intracellular Ca2+ level was highly associated with the change of membrane integrity (Figures 5 and 6) which could induce the opening of voltage-gated Ca^{2+} channels in the plasma membrane and the subsequent influx of Ca^{2+}. It has been largely considered that abnormal rise of cytosol Ca^{2+} is directly or indirectly responsible for a series of abnormalities within cells, which can damage cytoskeletal and membrane proteins, lipases, which can catalyze hydrolysis of membrane phospholipids, and endonucleases, which can cleave DNA.[36−39] Therefore, MMC-induced elevation of intracellular Ca^{2+} levels might play key roles in the final cytotoxicity of HPFs.

Conclusions

In conclusion, the results suggested that MMC could retard the growth of HPFs in a dose-dependent manner, and flow

cytometric analysis confirmed that the inhibitory effects of MMC on the growth of HPFs were associated with the involvement of apoptosis. We demonstrated that entrance of MMC into HPFs could cause changes of membrane characteristics as well as functions. All these changes were closely interrelated and can affect each other in turn, which may finally result in the disturbed cellular homeostasis and perhaps trigger the apoptotic signal pathway. This study indicates possible directions for exploration into the toxic mechanism of various environmental toxicants. However, more direct studies are further required to validate the interactions between MMC and the plasma membrane. At the same time, the results presented here also provide a new framework for the establishment of new experimental methods that incorporate AFM for visual studies of toxicity and for construction of visual trace drug screening models.

Acknowledgment. This work is supported by Ministry of Science and Technology of China (No.2010CB833603), the National Natural Science Foundation of China (No.60578025), and the Key Program of the National Natural Science Foundation of China (No. 30230350)

References and Notes

(1) Hofheinz, R. D.; Beyer, U.; Al-Batran, S. E.; Hartmann, J. T. *Onkologie* **2008**, *31*, 271–281.

(2) Todani, A.; Melki, S. A. *Int. Ophthalmol. Clin.* **2009**, *49*, 21–30.

(3) Rathore, P. K.; Kumari, S. P.; Pandey, R. M. *Orbital* **2009**, *28*, 297–302.

(4) Frederix, P. L.; Bosshart, P. D.; Engel, A. *Biophys. J.* **2009**, *96*, 329–38.

(5) Gaczynska, M.; Osmulski, P. A. *Curr. Opin. Colloid Interface Sci.* **2008**, *13*, 351–367.

(6) Muller, D. J. *Biochemistry* **2008**, *47*, 7986–7998.

(7) Parot, P; Dufrêne, Y. F.; Hinterdorfer, P.; Le Grimellec, C.; Navajas, D.; Pellequer, J. L.; Scheuring, S. *J. Mol. Recognit.* **2007**, *20*, 418–431.

(8) Cross, S. E.; Jin, Y. S.; Rao, J.; Gimzewski, J. K. *Nat. Nanotechnol.* **2007**, *2*, 780–783.

(9) Gaboriaud, F.; Dufrêne, Y. F. *Colloids Surf., B* **2007**, *54*, 10–19.

(10) Müller, D. J.; Helenius, J.; Alsteens, D.; Dufrêne, Y. F. *Nat. Chem. Biol.* **2009**, *5*, 383–390.

(11) Chaudhuri, O.; Parekh, S. H.; Lam, W. A.; Fletcher, D. A. *Nat. Methods.* **2009**, *6*, 383–388.

(12) Radmacher, M. *Methods Cell Biol.* **2007**, *83*, 347–372.

(13) Kuznetsova, T. G.; Starodubtseva, M. N.; Yegorenkov, N. I.; Chizhik, S. A.; Zhdanov, R. I. *Micron* **2007**, *38*, 824–833.

(14) Stolz, M.; Gottardi, R.; Raiteri, R.; Miot, S.; Martin, I.; Imer, R.; Staufer, U.; Raducanu, A.; Düggelin, M.; Baschong, W.; Daniels, A. U.; Friederich, N. F.; Aszodi, A.; Aebi, U. *Nat. Nanotechnol.* **2009**, *4*, 186–192.

(15) Titushkin, I.; Cho, M. *Biophys. J.* **2007**, *93*, 3693–3702.

(16) Li, Q. S.; Lee, G. Y.; Ong, C. N.; Lim, C. T. *Biochem. Biophys. Res. Commun.* **2008**, *374*, 609–613.

(17) Martens, J. C.; Radmacher, M. *Pflugers Arch.* **2008**, *456*, 95–100.

(18) Alcaraz, J.; Xu, R.; Mori, H.; Nelson, C. M.; Mroue, R.; Spencer, V. A.; Brownfield, D.; Radisky, D. C.; Bustamante, C.; Bissell, M. J. *EMBO J.* **2008**, *27*, 2829–2838.

(19) Hu, M. Q.; Chen, J. N.; Wang, J. K.; Wang, X. P.; Ma, S. Y.; Cai, J. Y.; Chen, Y.; Chen, Z. W. *J. Mol. Recognit.* **2009**, *22*, 516–520.

(20) Chen, Y.; Shao, L.; Ali, Z.; Cai, J. Y.; Chen, Z. W. *Blood* **2008**, *111*, 4220–4232.

(21) Jacobson, K.; Mouritsen, O. G.; Anderson, R. G. *Nat. Cell Biol.* **2007**, *9*, 7–14.

(22) Iyer, S.; Gaikwad, R. M.; Subba-Rao, V.; Woodworth, C. D.; Sokolov, I. *Nat. Nanotechnol.* **2009**, *4*, 389–393.

(23) Sergeev, I. N.; Li, S.; Ho, C. T.; Rawson, N. E.; Dushenkov, S. *J. Agric. Food Chem.* **2009**, *57*, 5771–5776.

(24) Dimitriadis, E. K.; Horkay, F.; Maresca, J.; Kachar, B.; Chadwick, R. S. *Biophys. J.* **2002**, *82*, 2798–2810.

(25) Brochu, H.; Vermette, P. *Langmuir* **2008**, *24*, 2009–2014.

(26) Bieling, P.; Laan, L.; Schek, H.; Munteanu, E. L.; Sandblad, L.; Dogterom, M.; Brunner, D.; Surrey, T. *Nature* **2007**, *450*, 1100–1105.

(27) Addae-Mensah, K. A.; Wikswo, J. P. *Exp. Biol. Med. (Maywood, NJ)* **2008**, *233*, 792–809.

(28) Schmitz, J.; Gottschalk, K. E. *Soft Matter* **2008**, *4*, 1373–1387.

(29) Lam, W. A.; Rosenbluth, M. J.; Fletcher, D. A. *Blood* **2007**, *109*, 3505–3508.

(30) Pelling, A. E.; Veraitch, F. S.; Chu, C. P.; Mason, C.; Horton, M. A. *Cell Motil Cytoskeleton* **2009**, *66*, 409–422.

(31) Chouinard, J. A.; Grenier, G.; Khalil, A.; Vermette, P. *Exp. Cell Res.* **2008**, *314*, 3007–3016.

(32) Park, J. E.; Yang, J. H.; Yoon, S. J.; Lee, J. H.; Yang, E. S.; Park, J. W. *Biochimie* **2003**, *84*, 1198–1204.

(33) Tyurina, Y. Y.; Tyurin, V. A.; Zhao, Q.; Djukic, M.; Quinn, P. J.; Pitt, B. R.; Kagan, V. E. *Biochem. Biophys. Res. Commun.* **2004**, *324*, 1059–1064.

(34) Ge, H.; Kong, X.; Shi, L.; Hou, L.; Liu, Z.; Li, P. *Cell Biol. Int.* **2009**, *33*, 402–410.

(35) Ye, H. Q.; Gan, L.; Yang, X. L.; Xu, H. B. *J. Ethnopharmacol.* **2006**, *103*, 366–371.

(36) Gong, Y.; Pan, X.; Huang, Y.; Gao, Z.; Yu, H.; Han, X. *Toxicol. Lett.* **2008**, *183*, 10–20.

(37) Tagliarino, C.; Pink, J. J.; Dubyak, G. R.; Nieminen, A. L.; Boothman, D. A. *J. Biol. Chem.* **2001**, *276*, 19150–19159.

(38) Wang, J. L.; Liu, C. S.; Lin, K. L.; Chou, C. T.; Hsieh, C. H.; Chang, C. H.; Chen, W. C.; Liu, S. I.; Hsu, S. S.; Chang, H. T.; Jan, C. R. *Toxicol. Lett.* **2005**, *160*, 76–83.

(39) Choi, J. H.; Lee, H. W.; Park, H. J.; Kim, S. H.; Lee, K. T. *Food Chem. Toxicol.* **2008**, *46*, 3486–3492.

JP910682Q